Physical and numerical modeling of infiltration in sand-geotextile systems

Siemens, G.A. and Bathurst, R.J.
GeoEngineering Centre at Queen's-RMC, Royal Military College of Canada, Civil Engineering Department, Kingston, Ontario, CANADA

Keywords: geotextile, unsaturated flow, capillary break, infiltration, geotextile water characteristic curves

ABSTRACT:
Geotextiles are widely used for filtration and separation in earth structures and are designed assuming saturated conditions. However in the field, geotextiles may exist in an unsaturated state for much of their life so these conditions should be accounted for in design. This paper describes experimental results and numerical simulations of unsaturated-saturated infiltration experiments on sand columns with a single geotextile layer inclusion. In the experiments, ponding pressure developed above the geotextile during infiltration. For numerical simulation calibration the hydraulic properties of the geotextiles were adjusted to reduce hydraulic conductivity function values. A parametric study was carried out using adjusted hydraulic values and a wide range of geotextile thickness and reference conductivity values. A unique relationship between ponding head and permittivity of the geotextile was found for the boundary conditions and sand material used.

1 INTRODUCTION

Geotextiles are widely used for filtration and separation functions in earth structures. In these applications, geotextiles are selected based on their Apparent Opening Size (AOS) or Filtration Opening Size (FOS) and saturated hydraulic conductivity (Holtz et al. 1997; Koerner 2005; CFEM 2006). However, in the field the selected geotextile may exist in an unsaturated state for much of its life. The result is large reductions in hydraulic conductivity that may significantly impact the performance of a geotextile as a filter or separator; thus the transient saturated-unsaturated hydraulic properties of geotextiles warrant investigation.

This paper describes the general approach and results of a set of numerical simulations that were carried out to predict the hydraulic behaviour of sand-geotextile columns. In order to get a reasonable match the hydraulic properties of the geotextiles were modified. This was attributed to the reduction in conductivity of the geotextiles due to soil particle penetration in the column tests that is not reproduced in conventional permittivity tests. The numerical simulation model with adjusted hydraulic parameters as the control data is used to carry out a numerical parametric study to quantify the influence of geotextile thickness, hydraulic conductivity and permittivity on 1-D ponding above a geotextile inclusion.

2 PHYSICAL TESTS

2.1 *Test Column and Methodology*

A schematic of the apparatus used to perform the sand and sand-geotextile infiltration tests is shown in Figure 1. The test methodology is reported in detail by Bathurst et al. (2007) and an expanded parametric study is presented in Siemens and Bathurst (2009). A control test with sand only and four tests with the same sand and a different single layer of geotextile were carried out. The sand was placed by pluviating through water. In the tests that included a geotextile, the geotextile was placed at a depth of 1200 mm. Following placement of the rest of the sand, the column was drained to the free water boundary. Infiltration tests began by applying 100 mm constant head at the surface. Progression of the water front was monitored using conductivity probes along the length of the column. Pore pressures were measured in the vicinity of the geotextile layer.

2.2 *Sand*

The sand (SP) used in the physical tests had a measured as-placed porosity of 0.52 and measured hydraulic conductivity of 2.0×10^{-3} m/s. The water retention values of the sand were measured using a Tempe cell. The Fredlund & Xing (1994) fitted curve for the wetting soil-water characteristic curve (SWCC) is plotted in Figure 2.

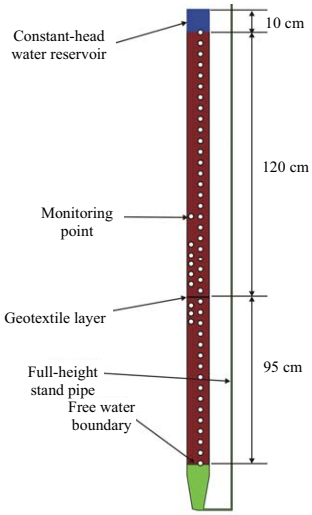

Figure 1. Schematic of the column numerical model geometry

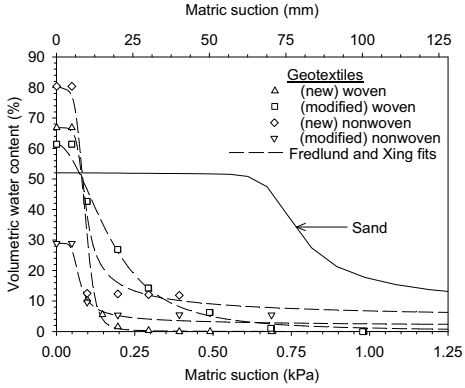

Figure 2. Wetting soil-water characteristic curve (SWCC) of sand and geotextile-water characteristic curves (GWCCs)

2.3 *Geotextiles*

Two typical commercially available geotextiles were used in the column tests. Properties used in the numerical simulations are given in Table 1. The geotextiles were subjected to index testing of compressibility, permittivity and water retention characteristics (Bathurst et al. 2007, 2009).

One material was a woven geotextile manufactured from polypropylene slit film monofilament. The second geotextile was nonwoven manufactured from continuous entangled polypropylene filament. To broaden the range of hydraulic properties the geotextiles were modified by the addition of a kaolin paste. Infiltration tests were carried out on sand columns with new and modified geotextile inclusions to create a wider range of geotextile-sand hydraulic response.

Table 1. Model parameters for new and modified woven and nonwoven geotextiles.

Parameter	New woven	Modified woven	New non-woven	Modified non-woven
Thickness, t_g (mm)	1.8	1.8	3.8	3.8
Porosity	0.72	0.64	0.86	0.32
Permittivity*, Ψ, (s^{-1})	0.0078	0.011	0.053	0.0024
Saturated hydraulic conductivity*, $K_{sat(geotextile)}$ (m/s)	2.0×10^{-5}	1.4×10^{-5}	2.0×10^{-4}	9.0×10^{-6}

Note: *adjusted values

For numerical simulations the relevant properties are the thickness, saturated hydraulic conductivity and geotextile-water characteristic curves (GWCCs). Geotextiles compress under vertical pressure. In the column tests, the geotextile inclusions were placed at 1200 mm below the surface. From one-dimensional compression tests performed on the geotextile specimens this depth corresponded to a thickness (t_g) of 1.8 mm and 3.8 mm for the woven and nonwoven geotextiles, respectively (Table 1).

The permittivity (Ψ) of the woven and nonwoven geotextile materials was measured in both new and modified conditions (Bathurst et al. 2009). The measured values were converted to hydraulic conductivity using

$$K_{sat}=\Psi\times t_g$$

where K_{sat} = saturated hydraulic conductivity in the direction normal to the plane of the geotextile (i.e. cross-plane direction).

GWCCs for the woven and nonwoven geotextiles in new and modified conditions were measured using a suction plate apparatus (Bathurst et al. 2009). The measured points and Fredlund & Xing (1994) fits for the wetting curves are shown in Figure 2.

3 PHYSICAL TEST RESULTS

Results from the physical infiltration column tests are shown in Figure 3. The pore-water pressure recorded by instrument T1 in the sand modified-nonwoven geotextile test remained constant at about -1.1 kPa from t = 0 to 130 s, while the wetting front was above the instrument elevation (Figure 3). Thereafter, T1 registered a sharp increase in pore-water pressure before stabilizing at a reading of about 0 kPa. The change in pore-water pressure from negative to 0 kPa was consistent with the wetting front breaking the initial capillary suction in the sand column which led to a higher level of saturation. A second jump in pore-water pressure occurred when the water front reached the geotextile layer at t = 160 s. The reason for the second jump in pore-pressure is due to the geotextile having lower hydraulic conductivity than the sand. In order to maintain water

front advance an increase in hydraulic gradient is required across the geotextile. In addition, a reduction in the water front progression was observed below the geotextile also due to a reduction in conductivity.

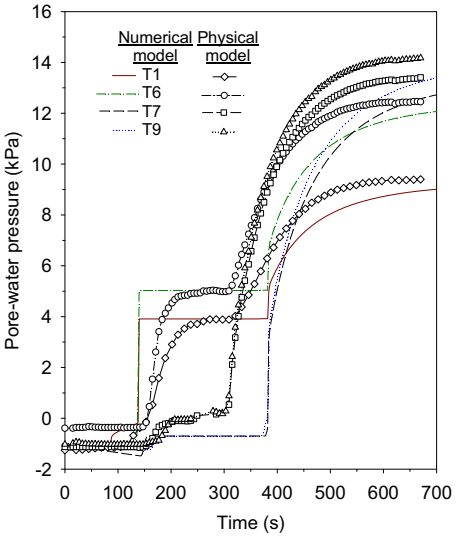

Figure 3. Measured and predicted pore-water pressures versus time for sand column with modified-nonwoven geotextile

When the wetting front reached the free water table at t = 310 s, the pore-water pressure at T1 increased rapidly toward the theoretical value of 9.4 kPa. It should be noted that the nonlinear pore-water pressure response with time after the infiltration front reaches the free-water boundary is due in part to the venting of air and flow of water into the manometer lines at the base and sides of the column.

Pore-water response curves for devices T7 and T9 located below the geotextile layer are also plotted in Figure 3. Qualitatively their response is the same as T1 except they only have one jump as they were placed below the geotextile.

For the other tests with a geotextile layer, the magnitude of the ponding was lowest for the new nonwoven geotextile with the highest saturated conductivity and greatest for the modified nonwoven geotextile with the lowest saturated conductivity.

4 NUMERICAL SIMULATIONS

The modeling approach was the same for all simulations in this investigation. Numerical calculations were performed using program SVFlux v5.10 (2004). The same model parameters were used for the sand above and below the geotextile. The model parameters for the GWCCs were applied to a thin region of the domain with the same geotextile thickness and elevation as the physical tests (Figure 1).

In order to match the measured pore-water pressures recorded by tensiometers as well as the water front advance with infiltration time, adjustment of some of the independently determined geotextile parameters were made (Table 1). The reasons for and the magnitude of parameter adjustments are described here. Using the measured permittivity, thickness values and derived saturated hydraulic conductivity of the geotextiles resulted in negligible ponding and little change in the rate of water front advance below the geotextile as was observed in the physical tests. In order to predict the measured ponding pressures the saturated hydraulic conductivity was reduced by up to two orders of magnitude for each geotextile. The reason for the required reduction in conductivity is attributed to intrusion of sand particles into the geotextile following placement in the column. The permittivity tests were performed in-isolation without soil surrounding the geotextile and are therefore upper bound values.

Results for the calibrated model are shown in Figure 3. In the sand modified-nonwoven geotextile column, the predicted pore pressures are consistent with measured values from 0-80 s. When the water front passes the T1 monitoring point, the pore pressure jumps and approaches 0 kPa. When the water front reaches the geotextile a second jump in pore pressure is recorded. In the numerical simulation the jump occurs over less than one second compared with 40-50 s in the physical tests. This may be attributed to compression of the air phase within the soil in the physical experiments as well as possible small delays in response time of the tensiometer devices (Bathurst et al. 2007). Similar jumps are noted at the monitoring points below the geotextile; thereafter, pore pressure remains constant until the water front reaches the free water boundary. At this point the stand pipe fills up and the pore pressure regime approaches hydrostatic conditions.

5 PARAMETRIC ANALYSIS

Following calibration, a parametric analysis was undertaken to examine the influence of geotextile properties on column response. Saturated hydraulic conductivity of the geotextiles was varied from 4×10^{-3} m/s to 9×10^{-6} m/s (e.g. $K_{sat(sand)}$ / $K_{sat(geotextile)}$ varied from 2 to 220). Geotextile thickness was varied from 0.8 mm to 9.8 mm. These ranges comprise a wide range of geotextile materials.

The parametric analysis results showed that both hydraulic conductivity and thickness of the geotextile influence column response. Therefore the influence of permittivity on hydraulic response of numerical columns was investigated. The numerical results are plotted in Figure 4 as maximum ponding

head versus permittivity using log-linear axes. In general, as permittivity deceases, maximum ponding head increases. Above a permittivity value of approximately $\Psi = 0.13\ s^{-1}$, no ponding is observed. Based on visual observation, a tri-linear approximation can be fitted to the data.

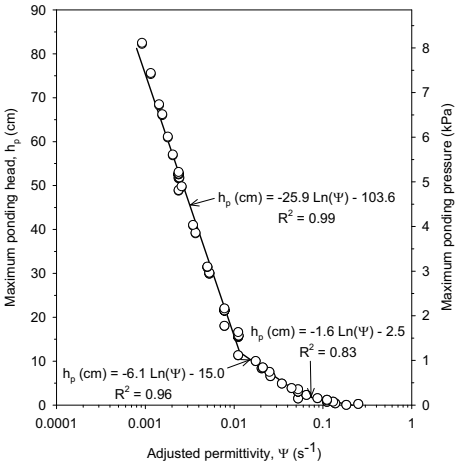

Figure 4. Maximum ponding head versus adjusted geotextile permittivity

The data in Figure 4 may be useful for the design of sand-geotextile systems subject to surface water infiltration loading when potential water ponding leading to horizontal migration of the water along the geotextile surface is undesirable (e.g. in reinforced soil walls). An expanded modeling study and general design chart are presented in Siemens and Bathurst (2009). A design methodology should proceed as follows: (1) scale index values of geotextile hydraulic conductivity; (2) estimate the insitu (compressed) geotextile thickness, and; (3) use Figure 4 to estimate the maximum ponding head under surface infiltration conditions.

Nevertheless, the quantitative conclusions made with respect to Figures 4 in this paper are likely valid only for the soil type, boundary conditions and configuration used in the physical and numerical models. Other soils with different particle size distributions, porosity and hydraulic conductivity can be expected to generate a different hydraulic response and hence a different ponding head-permittivity relationship. Therefore, different recommendations regarding a critical permittivity value will apply for other soil materials for design.

6 CONCLUSIONS

This paper presents results of selected physical tests and numerical simulations of 1-D infiltration tests on unsaturated sand and sand-geotextile columns. Input parameters used in numerical simulations were adjusted to improve the match between measured hydraulic response in physical column tests and predicted response. Numerical simulation results were consistent with physical test results by showing that a geotextile can cause a detectable delay in the progression of the water front below the geotextile and generate a sustained ponding head above the geotextile. The calibrated model is used to carry out a parametric analysis to investigate the influence of geotextile permittivity on potential water ponding over a geotextile layer in sand. For the range of geotextile parameters investigated in combination with a single sand type, the parametric study identified a minimum adjusted permittivity value above which ponding heights are negligible as well as a unique relationship between adjusted permittivity and maximum ponding head. Finally, quantitative results and conclusions must be restricted to the range of parameter values investigated in this study.

ACKNOWLEDGEMENTS

The work described in this paper was supported by grants awarded to the authors by the Natural Sciences and Engineering Research Council of Canada, the Academic Research Program at RMC, the Department of National Defence (Canada) and British Petroleum (formerly Amoco).

REFERENCES

Bathurst, R.J., Ho, A.F. and Siemens, G.A. 2007. A column apparatus for investigation of 1-D unsaturated-saturated response of sand-geotextile systems. *ASTM Geo. Test. J.,* Vol. 30(6), pp. 433-441.

Bathurst, R.J., Siemens, G.A. and Ho, A.F. 2009. Experimental investigation of infiltration ponding in one-dimensional sand-geotextile columns. *Geo. Int.,* Vol. 16(3), pp. 158-172.

Canadian Foundation Engineering Manual, 2006. Fourth Edition *Cdn Geot. Soc.*, Richmond, B.C, Canada, 488 p.

Fredlund, D.G. and Xing, A. 1994. Equations for the soil-water characteristics curve. *Cdn Geo. J.,* Vol. 31(4), pp. 521-532.

Holtz, R.D., Christopher, B.R. and Berg, R.R. 1997. Geosynthetic Engineering, *BiTech Publishers*, Richmond, British Columbia, Canada.

Koerner, R.M. 2005. Designing with Geosynthetics, Fifth Edition, *Prentice Hall*, Upper Saddle River, New Jersey, USA.

Ho, A.F. 2000. Experimental and numerical investigation of infiltration ponding in one-dimensional sand–geotextile columns. MSc thesis, *Queen's U.*, Kingston, ON, 212 p.

Siemens, G.A. and Bathurst, R.J. 2009. Numerical parametric investigation of infiltration in one-dimensional sand-geotextile columns. *Prov accptd to Geot & Geom* (#2053).

SVFlux v5.10. *SoilVision Systems Ltd.*, Saskatoon, Canada.